Controlled Amine Functionality in Self-Assembled Monolayers via the Hidden Amine Route: Chemical and Electronic Tunability

Yuval Ofir, Noemi Zenou, Ilya Goykhman, and Shlomo Yitzchaik*

Department of Inorganic and Analytical Chemistry & the HU Center for Nanoscience and Nanotechnology, The Hebrew University of Jerusalem, Jerusalem 91904, Israel

Received: December 12, 2005; In Final Form: February 14, 2006

A synthetic strategy for fabricating a dense amine functionalized self-assembled monolayer (SAM) on hydroxylated surfaces is presented. The assembly steps are monitored by X-ray photoelectron spectroscopy, Fourier transform infrared- attenuated total reflection, atomic force microscopy, variable angle spectroscopic ellipsometry, UV−vis surface spectroscopy, contact angle wettability, and contact potential difference measurements. The method applies alkylbromide−trichlorosilane for the fabrication of the SAM followed by surface transformation of the bromine moiety to amine by a two-step procedure: S_N2 reaction that introduces the hidden amine, phthalimide, followed by the removal of the protecting group and exposing the free amine. The use of phthalimide moiety in the process enabled monitoring the substitution reaction rate on the surface (by absorption spectroscopy) and showed first-order kinetics. The simplicity of the process, nonharsh reagents, and short reaction time allow the use of such SAMs in molecular nanoelectronics applications, where complete control of the used SAM is needed. The different molecular dipole of each step of the process, which is verified by DFT calculations, supports the use of these SAMs as means to tune the electronic properties of semiconductors and for better synergism between SAMs and standard microelectronics processes and devices.

Introduction

Self-assembled monolayers (SAMs) of organic molecules on various types of substrates have been studied extensively in the last years because of their possible applications ranging from nanotechnology fabrication techniques to fundamental surface science.[1] Alkylsiloxane SAMs[2] and alkanethiol SAMs[3] have emerged as the two types of most widely studied SAMs, where the first is applicable to hydroxyl baring surfaces and the second to metallic surfaces.

Organosilane SAMs have been widely applied to control surface properties such as hydrophobicity/hydrophilicity and surface charge/polarity,[4] for the fabrication of optically nonlinear materials,[5] as templates for growth of multilayer structures in the molecular layer epitaxy technique,[6] and as means for tuning the electronic properties of metals/semiconductors.[7]

The chemical functionality directed from the surface up has a crucial influence on the resulting surface properties and is used in turn for directing crystal growth,[8] as templates for the growth of conducting polymers such as polyaniline,[9] for applications in chromatography[10] and immobilization of molecules of interest such as single and double DNA strands,[11] enzymes, and antibodies,[12] and as a culturing substrate for neurons. In addition to their chemical functionalities, SAMs have been shown to be a promising method for micro- and nano-patterning through the application of various lithographic techniques.[13]

Of the many known organosilane SAMs, amino-terminated SAMs have been used frequently for the fabrication of patterned surfaces of biomolecules, such has enzymes[14] and peptides,[15] and selective electroless deposition of metals[16] and nanoparticles.[17] The chemical and physical natures of the aminosilylated thin layer are a consequence of the layer structure, ordering, and density and plays an important role in the utilization of the resulting layer in the above-mentioned uses. The reaction between silanol surface groups found on glass and silicon oxide substrates has been studied extensively by means of X-ray photoelectron spectroscopy (XPS) and near edge X-ray absorption fine structure,[18] spectroscopic ellipsometry,[19] diffuse reflectance Fourier transform spectroscopy,[20] solid-state ^{13}C NMR,[21] Kelvin probe force microscopy,[22] and attenuated total reflection Fourier transform infrared (FTIR-ATR) spectroscopy.[23]

The use of a precursor molecule that contains both the surface reactive group of chlorosilane and the amine functionality which could have been the ideal solution for the fabrication of an amine monolayer is not possible because of the reaction between the amine and chlorosilane moieties, and thus no such molecule exists. Most techniques used today for the fabrication of an amine-terminated SAMs are solution oriented and use chemisorption of aminoalkyl- and aminophenyl-functionalized alkoxysilanes on oxide-containing surfaces such as alumina, indium tin oxide, quartz, silica, glass, mica, or silicon dioxide.[24] The preparative route to silylated surfaces has a remarkable effect on the quality of the molecular layer. It affects the coating morphology which includes layer thickness, surface density, orientation of the surface molecules, and the type of interaction between the surface groups and the precursor molecules.[25] The presence of water has a significant influence on the mechanism of molecular layer formation and therefore on the structure of the deposited layer, especially with alkoxysilanes.[26] An immense problem in the fabrication of aminosilylated SAM on the surface of oxides is the acid−base interaction between the NH_2 headgroup of the precursor and the silanol groups on the

* Corresponding author. Phone: +972-2-6586971. Fax: +972-2-6585314. E-mail: sy@cc.huji.ac.il.

10.1021/jp057251k CCC: $30.25 © 2006 American Chemical Society
Published on Web 03/25/2006

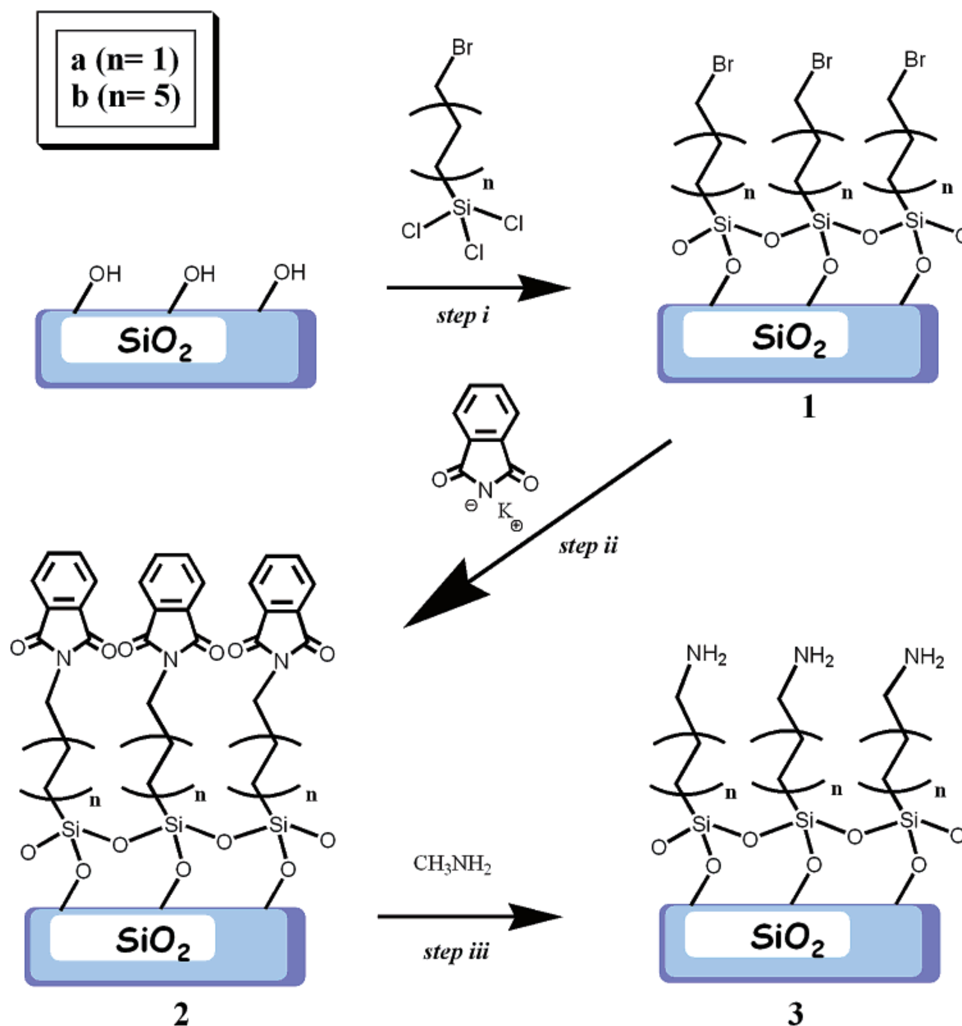

Figure 1. Modular synthetic route for the construction of amine-terminated SAMs.

surface,[27] resulting with molecules standing on their "head" and exposing the trialkoxysilane functionality to further react on the surface.

Silylated surfaces can be prepared in the gas or liquid phase; the latter case includes the sol−gel, aqueous, and organic solvent methods. The sol−gel synthesis results in a largely irreproducible product where the layer thickness and surface density of organosilanes cannot be precisely controlled. Furthermore, in the aqueous procedure at ambient conditions, uncontrolled condensation reactions result with an unpredictable thickness. The surface silanol groups hydrogen bond to the hydrolyzed alkoxy groups resulting in the formation of siloxane bonds and eventually leads to a three-dimensional (3D) polymeric network. It has been shown through theoretical calculations that in order to achieve a full, dense, and ordered monolayer, cross polymerization should be avoided.[28] Surface-saturated layers of aminosilanes can be deposited on silica under completely dry conditions, that is, in dried organic solvent or in the gas phase. The use of a gas phase reaction can therefore be beneficial, under which no solvents are needed and the precursor molecules which are possibly hydrolyzed cannot be vaporized at low deposition temperatures, resulting in a true monolayer structure. The vapor phase technique was first proposed by Haller[29] which showed deposition of (3-aminopropyl)triethoxysilane (APS) by heating a 5% solution of APS in toluene. The quality of the aminosilane SAMs produced by these methods has shown microstructural defects such as holes or aggregates.[30] Another methodology for the fabrication of a dense, true monolayer amine-functionalized SAM was developed by Sukenik and Balachander[24] and uses bromoalkyltrichlorosilane deposited on the surface which is then substituted in situ to azide followed by reduction to the free amine by $LiAlH_4$. In this method prolonged contact of the reducing agent with the SAM may result with damage to the SAM, or even precipitation of salt on top of the layer. An alternative methodology was developed by Dressick and Calvert[31] and uses photochemical transformation of an organized (*p*-chloromethyl)phenylsiloxane SAM by irradiation with 193 nm deep-UV light to aldehyde followed by reductive amination for the formation of an amine-terminated monolayer. This alternative route requires the use of deep-UV instrumentation and as already showed difficulties that are mostly connected to the time of exposure, leading to cleavage of Si−O and C−O bonds.[24]

To incorporate SAMs of various technologies, and especially amine-terminated SAMs which present a very versatile chemical accessibility, in standard microelectronics fabrication processes and harnessing these methods in the fabrication of new types of devices and especially in the field of molecular and organic electronics, there must be a complete compatibility between the processes, regarding the solvents, materials, and physical conditions during the deposition. Therefore there is a need for a simple and accessible (in chem. labs) synthetic route to amine-containing SAMs with a defined and exact structure. The procedure we chose for the fabrication of a dense, amine-functionalized SAM is based on hidden amine functionality inside the layer (Figure 1). The phthalimide, which is found as

protecting group at Gabriel synthesis procedures,[32] seems small enough and can form π-stacking and therefore was chosen as a candidate for the process. The strategy uses the protection group not in the process of the deposition of the layer because the bulky precursor damages the density of the resulting layer as was already shown by Grunze.[33] Our methodology is modular and first uses a (3-bromoalkyl)trichlorosilane, a precursor which is known to from an ideal and dense SAM, substitution the bromine with a hidden amine by S_N2 reaction, followed by hydrolysis to yield the free amine. The resulting monolayer retains the density of the original trichlorosilane SAM, but with a complete altered functionality, the amine.

It is widely appreciated that the work function (Φ), the minimum energy required for an electron to escape into vacuum from the Fermi level (E_F) of a substrate depends on the conditions of the surface, both morphologically and chemically. Adsorption of molecules or atoms on a metal/semiconductor surface can affect the electronic properties of the surface in several ways. In principle the straightest effect is that of a molecular dipole on work function. Recently Kobayashi[34] has shown to be able to control the carrier density in the conduction channel of an organic field effect transistor by the use of SAMs with a different terminal group that is characterized by a different molecular dipole. Another work reported by Cahen,[35] has shown that the effective barrier height of n-type GaAs semiconductor diodes can be tuned by using a series of multifunctional molecules whose dipole is varied systematically.

The different stages of our proposed process are also characterized by a different dipole moment of the SAM (due to the changed functionality) and thus present an added advantage to our methodology and allow control over the surface electronic properties, as is shown by the CPD measurements.

Materials and Methods

(A) General. (1) Substrate Cleaning. Quartz (Chemglass) and n-Si ⟨100⟩ (Virginia Semiconductors) substrates were cleaned in aqueous detergent, rinsed copiously with triple distilled water (TDW), in hot (90 °C) piranha solution for 30 min (3:7 by volume of 30% H_2O_2 and H_2SO_4, *caution: strong oxidizing solution, handle with care*). The substrates were then rinsed with TDW and further cleaned with $H_2O/H_2O_2/NH_3$ (5:1:0.25) solution while sonicating for 5 min at 60 °C. After subsequent washing with TDW, the substrates were immersed for 5 min in pure acetone and then in pure methanol and finally dried under a stream of nitrogen.

(2) Chemicals. (a) Coupling Agents. (11-Bromoundecyl)-trichlorosilane (BUTCS) and (3-bromopropyl)trichlorosilane (BPTCS) were purchased from Gelest and vacuum distilled before use.

(b) Solvents. *n*-Hexane, toluene, and dimethylformamide (DMF) were distilled and dried on sodium under nitrogen atmosphere. HCl, H_2O_2, and 2-propanol were purchased from J. T. Baker and used as received.

(c) Reagents. Potassium phthalimide, methylamine 40% in water, and sodium borohydride were purchased from Aldrich and used as is.

(B) SAM Preparation. (1) Brominated Monolayer Preparation. SAMs of BPTCS (**1a**) and BUTCS (**1b**) were formed by immersing freshly cleaned Si/SiO_2 (silicon's native oxide) or quartz substrates in a 1% (v/v) hexane/toluene solution respectively for 20 min under inert conditions in a Schlenk line system. Upon completion of the reaction, the substrates were washed three times with toluene/hexane, sonicated for 1 min in acetone in order to remove any excess of coupling agent, and allowed to dry in an oven at 110 °C.

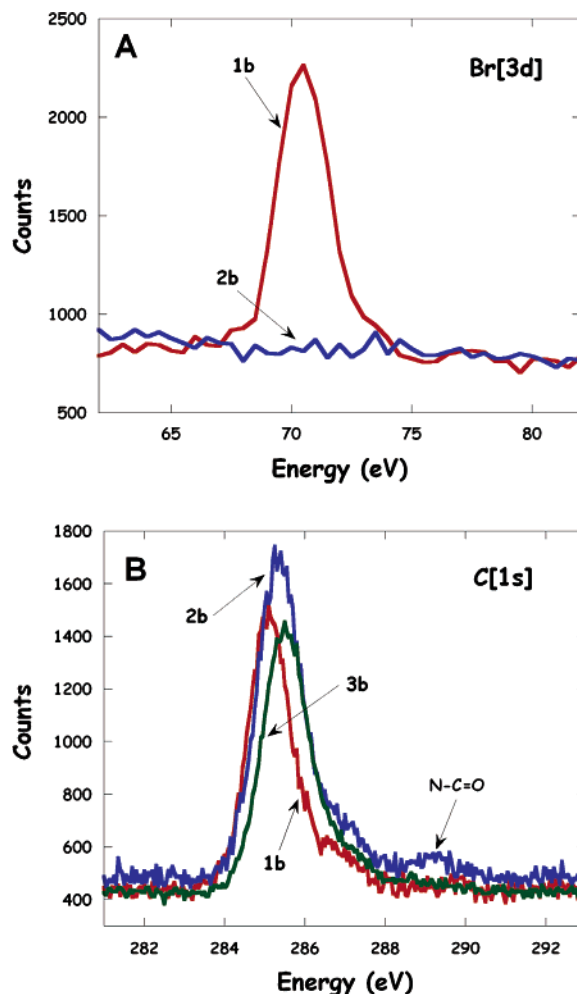

Figure 2. XPS spectra of the substitution reaction of **1b** to **2b** (see, step ii, Figure 1): (A) bromine spectral region; (B) carbon spectral region.

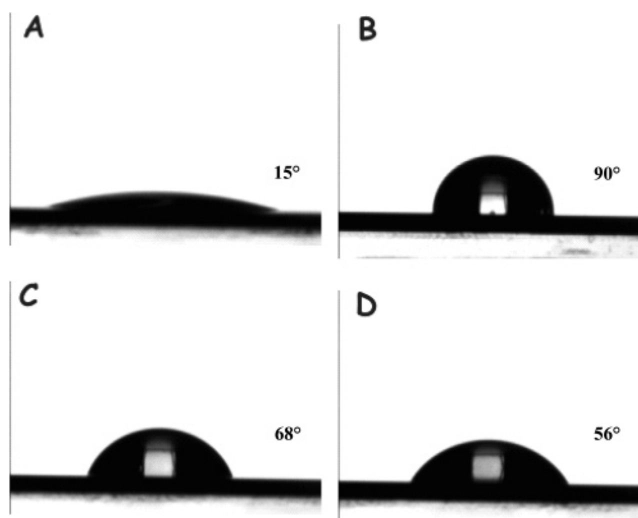

Figure 3. Water contact angle on a clean Si/SiO_2 surface (A) and on undecyl-based SAMs: **1b** (B), **2b** (C), and **3b** (D).

(2) Monolayer Functionalization to Phthalimide. SAMs **1a** and **1b** were modified by dipping the substrates for 3 h in dry DMF 18 mM potassium phthalimide solution at 60 °C under inert conditions. Upon completion of the reaction, the substrates were washed with DMF, DMF/TDW water mixture, and TDW,

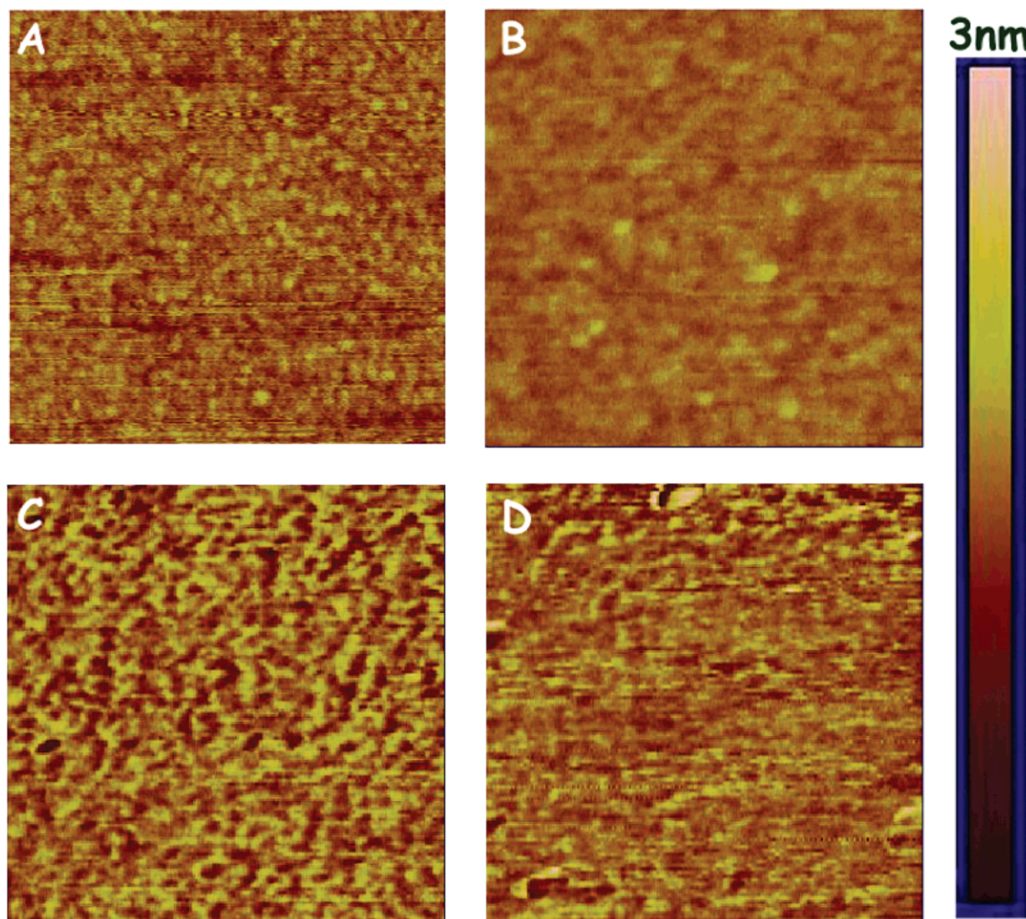

Figure 4. AFM images of clean Si/SiO_2 surface (A) and on undecyl-based SAMs: **1b** (B), **2b** (C), and **3b** (D) (images are 1 μm × 1 μm).

sonicated for 1 min in 2-propanol, and finally dried under nitrogen flow.

(3) Monolayer Functionalization to Amine. SAMs **2a** and **2b** were immersed in 40% methylamine in water for 1 min, washed with TDW and DMF/TDW mixture, sonicated in 2-propanol for 5 min, and finally dried under nitrogen flow.

(C) Instrumentation. Atomic force microscopy (AFM) measurements were carried out with a Nanoscope IV (DI) in tapping mode using a tapping etched silicon probe (TESP, DI) with a 30 N/m force constant. All substrates were imaged in air. UV−vis spectra were acquired on a Shimadzu UV-3101PC spectrophotometer using quartz substrates. Contact angle measurements were performed using Si substrates with a FTA125 video-based contact angle meter (First Ten Ångstroms). XPS spectra were collected at ultrahigh vacuum (2.5×10^{-10} Torr) on a 5600 Multi-Technique (AES/XPS) system (PHI) using an X-ray source of Al Kα (1486.6 eV). Variable-angle spectroscopic ellipsometry (VASE) measurements were carried out on a VB-200 ellipsometer (Woollam Co.) around the Brewster angle of Si (75°). FTIR-ATR measurements were done on a Nicolet 740 spectrophotometer equipped with a mercury cadmium telluride detector cooled by liquid nitrogen, using 500 scans for each spectrum. Double-side polished single-crystal silicon was used as a substrate for these measurements with dimensions of 5 cm × 1 cm × 0.5 cm which allowed about 100 internal reflections inside the substrate. Contact potential difference (CPD) measurements[36] were made with a commercial instrument, Kelvin probe S (DeltaPhi Besocke, Jülich, Germany), equipped with a vibrating gold electrode (work function 5.1 eV) at ambient conditions in a home-built Faraday cage.

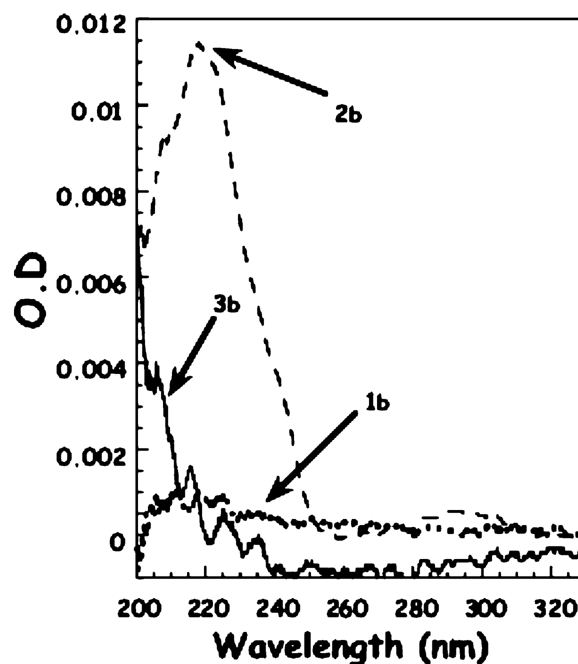

Figure 5. UV−vis absorption spectra of the BUTCS SAM at various steps of the surface reactions.

(D) Calculations. Dipole moments and molecular length for the various models of molecules were calculated by the B3LYP (Becke three-parameter hybrid exchange[37] with Lee−Yang−Parr correlation)[38] density functional theory (DFT) method using the Gaussian 98 program package[39] that incorporates electron

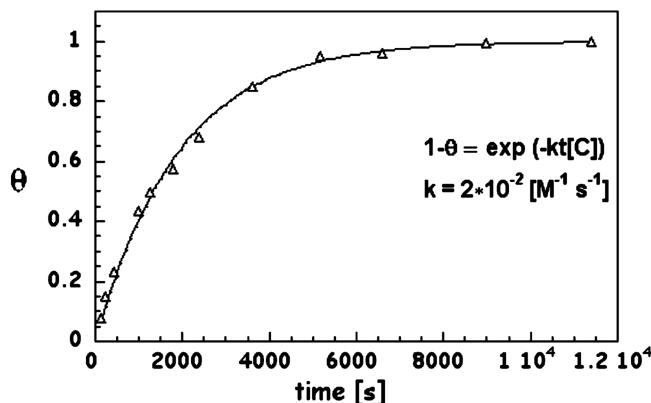

Figure 6. Phthalimide surface coverage (calculated from UV−vis absorption at 220 nm) change as a function of time during the S_N2 reaction of **1b** SAM. Insert: reaction rate equation and rate constant.

correlation, using the contracted basis set cc-pVDZ (correlation consistent polarized valence double-ζ).[40] Visualization of the molecules and the calculated dipole moment is done using Molekel, version 4.3, available free on the Internet.[41]

Results and Discussion

The quality and buildup of **1a** and **1b** bromoalkyl monolayers (Figure 1, step i) is clear from the Br[3d] XPS peak at 69.1 eV (Figure 2A) found in bromoalkanes. CA changes from 15° for the bare SiO_2 to 75° and 90° for **1a** and **1b** respectively (Figure 3B). Ellipsometric VASE measurement at an incidence angles of 70°/75°/80° showed a thickness of 6 (±0.3) Å for **1a** and 14 (±1) Å for **1b** (a Cauchy model was used as a model for fitting the experimental data, using a refractive index of 1.45 for the organic SAM) which are comparable to the calculated length of 5.2 Å for a bromopropyl and a length of 14.4 Å for a bromoundecyl segment. AFM imaging after the coupling reaction shows a very smooth surface with an root mean square (rms) roughness of 1.1 Å (Figure 4B), thus confirming there is no polymerization of the coupling agent.

The second stage of the process involves the introduction of the phthalimide protecting group by substitution with the bromine atom and the removal of KBr salt (Figure 1, step ii). The substrates were immersed for 3 h in dry 18 mM potassium phthalimide DMF solution under inert conditions. The substitution was followed by monitoring the XPS of the substituted substrate, which shows disappearance of the Br[3d] peak at 69.1 eV (Figure 2A), the appearance of the N[1s] signal at 398.5 eV, and a shoulder typical of the C[1s] in the carbonyl moiety of the phthalimide at 288.4 eV (Figure 2B). The disappearance of the Br[3d] peak shows a conversion of nearly 100%, which is very important for the next step (the removal of the phthalimide to get the free amine). The XPS spectrum was also scanned at the range of 295 eV which is characteristic to the K[2p]. The absence of a peak in this region proves there are no traces of potassium on the surface. The presence of the phthalimide group is also verified by a change in the CA from 75° to 55° for the **1a** monolayer, and from 90° to 68° for the **1b** monolayer (Figure 3C). The UV−vis absorption spectrum shows a new absorption peak at 220 nm characteristic of the phthalimide moiety (Figure 5). This spectroscopic footprint enabled us to follow the kinetics of the substitution reaction between the bromine and the phthalimide as depicted in Figure 6. The process follows first-order kinetics (inset Figure 6) where θ is the surface coverage. The kinetics shows that after 2 h all the bromine was substituted with phthalimide. Learning the time scale for the process allows controlling the degree of the substitution reaction and in turn obtaining a mixed-monolayer system with more then one functionality, for example a 50/50 ratio between NH_2 and Br functionalities was achieved following 21 min reaction time. The fabrication of mixed monolayers has already been shown to be very useful in binding macromolecules,[42] and this technique could prove to be very useful in this field. AFM imaging of the surface after the substitution reaction is shown in Figure 4C and shows a clean and flat surface with an rms roughness of 2.9 Å and a slightly different morphology than the bromine-functionalized layer. IR-ATR measurements preformed on the **1b**−phthalimide layer prove the existence of the phthalimide, by showing the stretching vibrations of 11 methylene groups of the undecyl moiety at 2923 and at 2853 cm^{-1} and a stretching vibration characteristic of the phthalimide's carbonyl moiety at 1717 cm^{-1} (Figure 7).

When attempts were made to remove the phthalimide moiety to reveal the free amine, a few methods were considered: acidic hydrolysis[43] by refluxing in HCl 20% and then adding base to get the free amine; use of methylamine[44] for a two step

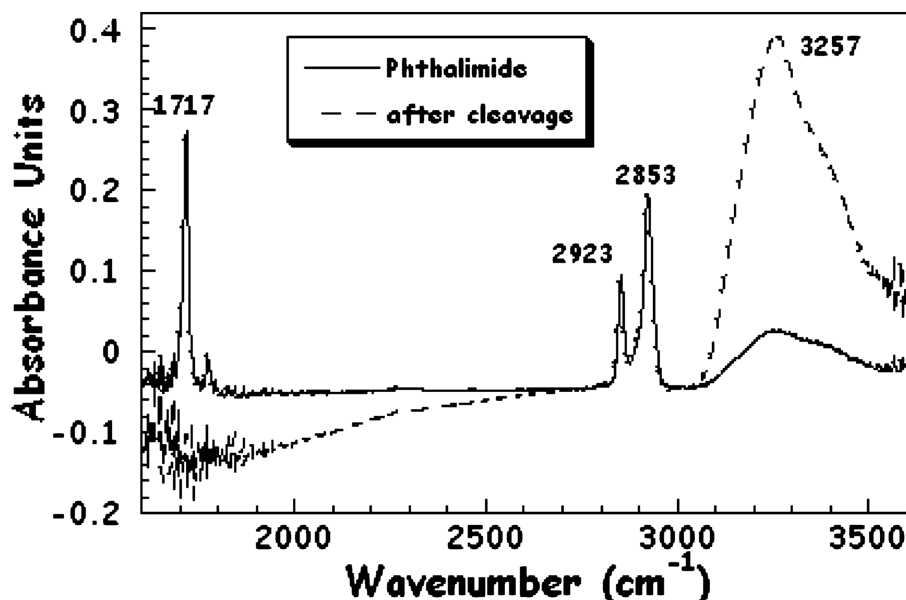

Figure 7. IR-ATR spectra for **2b** (full line) and **3b** (dashed line) SAMs.

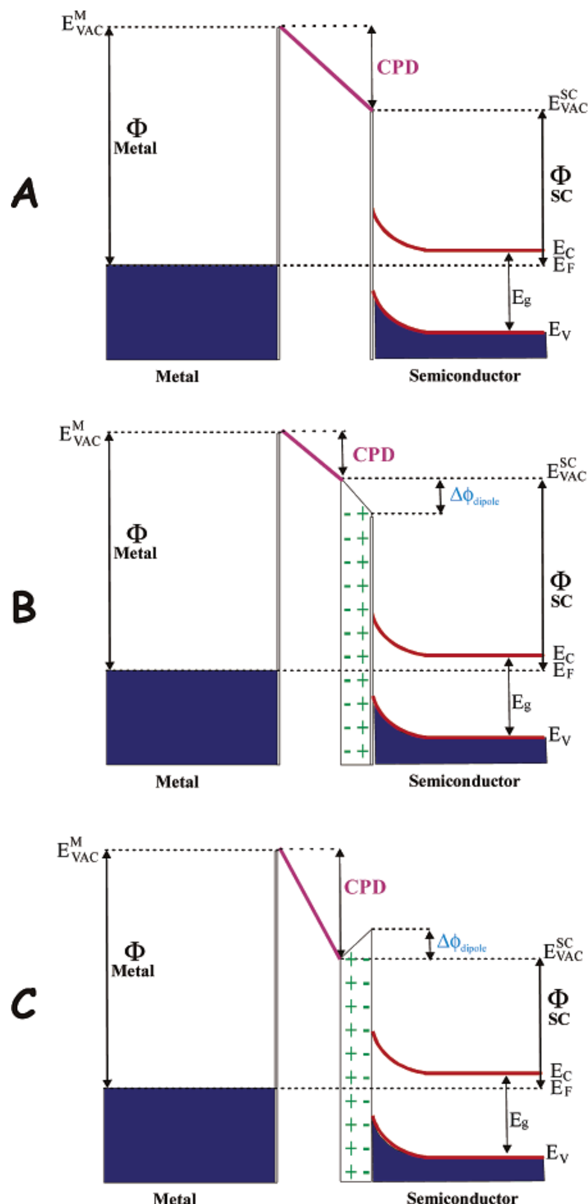

Figure 8. Schematic description of the change in the CPD of a semiconductor upon deposition of dipole film in reference to a metal probe (Au, work function 5.1 eV) in three possibilities: (a) no dipole layer; (b) dipole pointing away from the surface; (c) dipole pointing toward the surface.

hydrolysis; use of $NaBH_4$/2-propanol.[45] All techniques proved to be harmful to the **1a** derived monolayer and resulted in partial to complete removal of the monolayer from the surface and even harsh damage to the surface in the case of sodium borohydride. The methylamine technique proved to be useful for the removal of the phthalimide protecting group in the case of the **1b** monolayer as is seen from the absorption spectrum (Figure 5). The CA changes from 68° to 56° (Figure 3D), a value comparable to results of other $C_{11}-NH_2$ layers fabricated by other techniques.[46] The VASE derived ellipsometric thickness after the removal of the protecting group was reduced by 2 Å compared to the thickness with the protecting group. We attribute the smaller than expected thickness reduction to a different packing orientation. Past the hydrolysis no apparent IR vibration is seen at 1717 cm^{-1} while a new wide vibration characteristic of the free amine appears at 3200 cm^{-1}. Also present are the stretching vibration characteristic for the CH_2 at 2923 and at 2853 cm^{-1} which proves that the alkyl monolayer

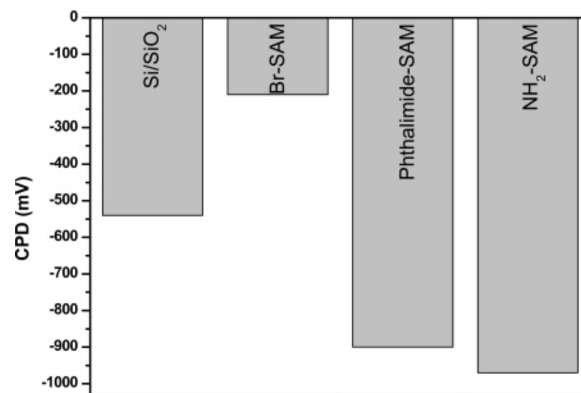

Figure 9. The change in CPD as a function of terminal group on BUTCS SAM compared to a vibrating gold electrode (experimental accuracy ±35 meV).

is kept unharmed. AFM imaging of the free amine monolayer again resulted with a flat and clean layer having a rms roughness of 2.4 Å (Figure 4D).

The effect of the different molecular dipoles, characteristic of the different process stages, on the work function of highly doped Si substrates was studied using CPD measurements. The work function of a semiconductor is determined by three factors (Figure 8): (i) the electron affinity (EA), the energy needed to bring an electron from vacuum just outside the semiconductor to E_V at the surface; (ii) the band bending (BB), the electrical potential difference between the surface and the electrically neutral semiconductor bulk, often called the *built-in potential*, expressed in the band diagram by bending of E_V and E_C near the surface; (iii) the energy difference between the Fermi level and E_C in the bulk. Since our "molecular spacer" (the alkyl chain) in the three stages stays the same throughout all the process, there is no real change in the BB (which is associated with the number of surface states/traps, i.e., the passivation of the surface with the SAM) at the different steps, and we can attribute the change in the CPD or work function only to the change in EA. The change in EA is directly related to the molecular dipole size and direction of the molecules comprising the SAM (Figure 8). The effect of the dipole on the measured surface potential can be extracted from the Helmholtz[47] relation

$$\Delta\Phi = \frac{N\mu \cos\theta}{\epsilon\epsilon_0} \qquad (1)$$

where N is the dipole density (per square centimeter), μ is the dipole moment (in debyes),[48] θ is the *average* angle of the dipole with respect to the surface normal, ϵ is the effective dielectric constant of the molecular film,[49] and ϵ_0 is the permittivity of vacuum.[50]

The CPD measurements of the BUTCL-based SAMs are shown in Figure 9. While there is a change in the BB of the substrate after the deposition of the Br-terminated BUTCS layer, this change is of about 50−60 meV, as determined by others.[7c] The measurements show a decrease of the substrate work function after the deposition of the brominated layer, and an increase of the substrate work function for the phthalimide- and amine-terminated BUTCS-based SAMs. To verify the tendency in the CPD results, the molecular dipoles of a series of molecules that model the molecules on the surface were calculated using Gaussian 98 (Figure 10 and Table 1). The direction of the dipole moment of the bromine and phthalimide functional groups directed from the interface is completely opposite and that of the phthalimide and amine is the same (the direction but not

TABLE 1: Experimental Results of the Change in Surface Potential and Extrapolated Dipole Moment vs Calculated Values of Dipole Moment

molecule	measured change in work function[a] (eV) ±30 meV	calculated total dipole[b] (D)	calculated dipole along molecular axis[b] (D)	calculated dipole along normal axis[c] (D)	measured dipole along normal axis[d] (D)
Br−undecyl	0.33	2.3833	2.2471	2.0365	0.6
Ph−undecyl	−0.36	2.3813	−1.9499	−1.7672	−0.65
NH_2−undecyl	−0.43	1.1691	−0.2758	−0.2499	−0.78
NH_3−undecyl		29.5527	−29.5401	−26.7724	

[a] Experimentally derived from $CPD_{SAM} - CPD_{BARE}$. [b] Calculated using Gaussian 98 (see text on calculations). [c] Calculated by multiplication of the dipole along the molecular axis with cos θ (θ being the tilt angle, and considered to be 25°). [d] Calculated from eq 1 where $N = 4 \times 10^{18}$ (molecules/m^2), μ (1 D = 3.336×10^{-30} C m), $\epsilon = 2.5$ (see ref 49), and $\epsilon_0 = 8.854 \times 10^{-12}$ ($C^2\ m^{-1}\ J^{-1}$).

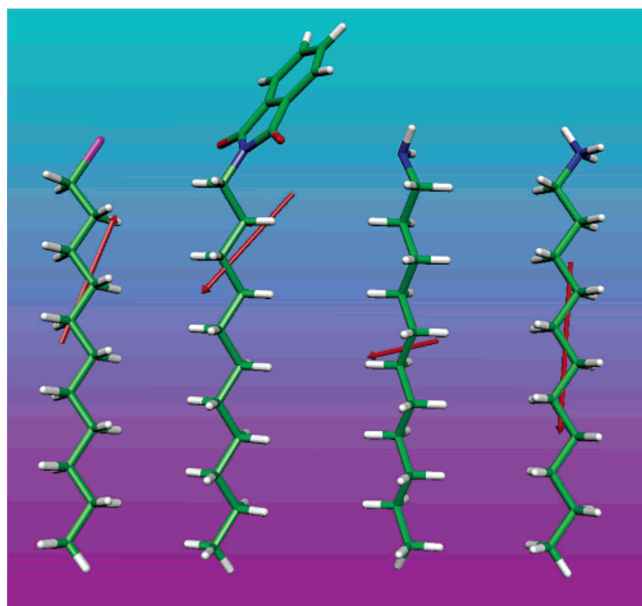

Figure 10. Visualization of the molecular dipoles (dipole pointing from positive to negative) built from the Gaussian 98 output file using the "Molekel" software. From left to right: Br−undecyl, phthalimide−undecyl, amine−undecyl, and protonated amine−undecyl (the magnitude of the dipole moment of the protonated amine−undecyl is scaled to 10% in order to fit the figure).

the magnitude). The molecular dipole calculated for the free molecule is a vector in 3D, but when considering the effective dipole moment in regard to the surface work function, only the perpendicular component of the dipole is relevant (see Table 1). The change in the CPD holds well with the calculated perpendicular dipole of the free molecules both for the Br-terminated molecule and for the phthalimide-terminated molecule but at first glance falls for the amine-terminated molecule. The calculated dipole for the amine-terminated molecule is too small to account for the large change (−0.43 eV) in the CPD, an even higher change then that of the phthalimide−SAM. This discrepancy in the results can be explained by a partially charged/protonated amine layer, as was reported by others.[51] The reported amount of protonation (i.e., ammonium group) in these kinds of SAMs can go up to 20% and can thus change the effective dipole of the layer. Calculations preformed on a protonated molecule show a huge increase in the molecular dipole up to ∼30 D (see Table 1). Considering a 10% protonation in the SAM brings the average effective dipole to about 2.9 D.

Conclusions

We presented a new approach for obtaining a SAM with amine functionality on hydroxylated surfaces using the formation of a dense monolayer of alkylbromide−trichlorosilane and transformation of the bromine moiety to amine by a two-step procedure, S_N2 reaction with phthalimide followed by the transformation to the free amine. The technique has proven useful for obtaining an amine-terminated SAM based on the BUTCS but fails to do so for the BPTCS-derived SAM. This difference is ascribed to the less ordered and less dense SAM formed by BPTCS, thus making it less durable to the basic environment at the last step of the reaction, resulting in a partial or complete removal of the SAM. The reported method holds a few advantages compared to the method developed by others, which are mainly the shorter substitution time of the bromine with phthalimide rather than with azide (3 h compared to 24 h), the removal of the protecting phthalimide group takes less than a minute while the reduction of the azide to amine takes 16 h, and in our case the hydrolysis is done in a basic environment so there is no need to add base at the end to get the free amine. Controlled removal of the protecting group allows mixed functionality containing monolayers that have a lot of importance in tuning chemical functionality on surfaces. The different dipole moment, characteristic for each layer and especially that of the Br/phthalimide SAM can potentially be used to tune the electronic properties of surfaces and be used in optimization/enhancement of standard microelectronic devices and organic-materials based devices. This method is chemically compatible with standard microelectronics fabrication techniques and therefore paves the way for a stronger combination of SAMs in standard microelectronics and molecular nanoelectronics.

Acknowledgment. S.Y. thanks the Israel Science Foundation (Grant 225/99-1) and the European Commission Grant for Future and Emerging Technologies, No. IST-2001-38951, for financial support. Y.O. and N.Z. thank the Israel Ministry of Science for Eshkol Ph.D. scholarship. Y.O. thanks J. Ghabboun for helpful discussions and D. Schweke for help in DFT calculations.

References and Notes

(1) Ulman, A. *Chem. Rev.* **1996**, *96*, 1533−1554.

(2) Sagiv, J. *J. Am. Chem. Soc.* **1980**, *102*, 92−98.

(3) Nuzzo, R.; Allara, D. *J. Am. Chem. Soc.* **1983**, *105*, 4481−4483.

(4) (a) Plueddemann, E. P. In *Silane Coupling Agents*; Plenum: New York, 1991. (b) *Silanes and Other Coupling* Agents; Mittal, K. L., Ed.; VSP: Leiden, The Netherlands, 1992. (c) Ulman, A. In *An Introduction to Ultrathin Organic Films from Langmuir−Blodgett to Self-Assembly*; Academic Press: New York, 1991.

(5) Yitzchaik, S.; Marks, T. J. *Acc. Chem. Res.* **1996**, *29*, 197−202.

(6) (a) Burtman, V.; Zelichenok, A.; Yitzchaik, S. *Angew. Chem., Int. Ed.* **1999**, *38*, 2041−2045. (b) Burtman, V.; Ofir Y.; Yitzchaik, S. *Langmuir* **2001**, *17*, 2137−2142.

(7) (a) Cohen, R.; Zenou, N.; Cahen, D.; Yitzchaik, S. *Chem. Phys. Lett.* **1997**, *279*, 270−274. (b) Ray, S. G.; Cohen, H.; Naaman, R.; Liu, H.; Waldeck, D. H. *J. Phys. Chem. B* **2005**, *109*, 14064−14073. (c) Gershewitz, O.; Grinstein, M.; Sukenik, C. N.; Regev, K.; Ghabboun, J.; Cahen, D. *J. Phys. Chem. B* **2004**, *108*, 664−672.

(8) (a) Aizenberg, J.; Black, A. J.; Whitesides, G. M. *Nature* **1999**, *398*, 495−498. (b) Travaille, A. M.; Kaptijn, L.; Verwer, P.; Hulsken, B.; Elemans, J. A. A.; Nolte, W. R. J. M.; van Kempen, H. *J. Am. Chem. Soc.* **2003**, *125*, 11571−11577.

(9) Sfez, R.; De-Zhong, L.; Turyan, I.; Mandler, D.; Yitzchaik, S. *Langmuir* **2001**, *17*, 2556−2559.

(10) Trammell, B.; Ma, C. L.; Luo, H.; Jin, D.; Hillmyer, M. A.; Carr, P. W. *Anal. Chem.* **2002**, *74*, 4634−4639.

(11) Aqua, T.; Naaman, R.; Daube, S. S. *Langmuir* **2003**, *19*, 10573−10580.

(12) (a) Culha, M.; Stokes, D.; Allain, L. R.; Vo-Dinh, T. *Anal. Chem.* **2003**, *75*, 6196−6201. (b) Qian, X.; Metallo, S. J.; Choi, I. S.; Wu, H.; Liang, M. N.; Whitesides, G. M. *Anal. Chem.* **2002**, *74*, 1805−1810. (c) Oren, R.; Sfez, R.; Korbakov, N.; Shabtai, K.; Cohen, A.; Erez, H.; Dormann, A.; Cohen, H.; Shappir, J.; Spira, M. E.; Yitzchaik, S. *J. Biomater. Sci., Polym. Ed.* **2004**, *15*, 1355−1374.

(13) (a) Lee, B.-w.; Clark, N. A. *Langmuir* **1998**, *14*, 5495−5501. (b) Saito, N.; Hayashi, K.; Sugimura, H.; Takai, O. *Langmuir* **2003**, *19*, 10632−10634. (c) Hong, L.; Sugimura, H.; Furukawa, T.; Takai, O. *Langmuir* **2003**, *19*, 1966−1969. (d) Sugimura, H.; Hanji, T.; Hayashi, K.; Takai, O. *Ultramicroscopy* **2002**, *91*, 221−226. (e) Lee, W.; Kim, E. R.; Lee, H. *Langmuir* **2002**, *18*, 8375−8380. (f) Piner, R. D.; Zhu, J.; Xu, F.; Hong, S. H.; Mirkin, C. A. *Science* **1999**, *283*, 661−663. (g) Liu, G. Y.; Xu, S.; Qian, Y. *Acc. Chem. Res.* **2000**, *33*, 457−466. (h) Hoeppener, S.; Maoz, R.; Sagiv, J. *Nano Lett.* **2003**, *3*, 761−767.

(14) Sugimura, H.; Nakagiri, N. *J. Am. Chem. Soc.* **1997**, *119*, 9226−9229.

(15) Amoa, I. B.; Sutherland, T. C.; Li, C. Z.; Silerova, R.; Kraatz, H. B. *J. Phys. Chem. B* **2004**, *108*, 704−714.

(16) (a) Azzaroni, O.; Schilardi, P. L.; Salvarezza, R. C. *Electrochim. Acta* **2003**, *48*, 3107−3114. (b) Hoeppener, S.; Maoz, R.; Cohen, S. R.; Chi, L.; Fuchs, H.; Sagiv, J. *Adv. Mater.* **2002**, *14*, 1036−1041.

(17) Liu, S.; Maoz, R.; Schmid, G.; Sagiv, J. *Nano Lett.* **2002**, *2*, 1055−1060.

(18) (a) Kallury, K. M. R.; MacDonald, P. M.; Thompson, M. *Langmuir* **1994**, *10*, 492−499. (b) Bierbaum, K.; Kinzler, M.; Woll, Ch.; Grunze, M.; Hahner, G.; Heid, S.; Effenberger, F. *Langmuir* **1995**, *11*, 512−518. (c) Kallury, K. M. R.; Krull, U. J.; Thompson, M. *Anal. Chem.* **1988**, *60*, 169−172. (d) Sugimura, H.; Hozumi, A.; Kameyama, T.; Takai, O. *Surf. Interface Anal.* **2002**, *34*, 550−554.

(19) Moon, J. H.; Shin, J. W.; Kim, S. Y.; Park, J. W. *Langmuir* **1996**, *12*, 4621−4624.

(20) (a) Ek, S.; Iiskola, E. I.; Niinisto, L.; Vaittinen, J.; Pakkanen, T. T.; Keranen, J.; Auroux, A. *Langmuir* **2003**, *19*, 10601−10609. (b) Ek, S.; Iiskola, E. I.; Niinisto, L. *Langmuir* **2003**, *19*, 3461−3471.

(21) Blumel, J. *J. Am. Chem. Soc*. **1995**, *117*, 2112−2113.

(22) (a) Hayashi, K.; Saito, N.; Sugimura, H.; Takai, O.; Nakagiri, N. *Ultramicroscopy* **2002**, *91*, 151−156. (b) Sugimura, H.; Hayashi, K.; Saito, N.; Nakagiri, N.; Takai, O. *Appl. Surf. Sci.* **2002**, *188*, 403−410.

(23) Rudkevich, E.; Savage, D. E.; Cai, W.; Bean, J. C.; Sullivan, J. S.; Nayak, S.; Kuech, T. F.; McCaughan, L.; Lagally, M. G. *J. Vac. Sci. Technol., A* **1997**, *15*, 2153−2157.

(24) (a) Kleinfeld, D.; Kahler, K. H.; Hockberger, P. E. J. *J. Neurosci.* **1988**, *8*, 4098−4120. (b) Dulcey, C. S.; Georger, J. H.; Krauthamer, V.; Stenger, D. A.; Fare, T. L.; Calvert, J. M. *Science* **1991**, *252*, 551−554. (c) Stenger, D. A.; Georger, J. H.; Dulcey, C. S.; Hickman, J. J.; Rudolph, A. S.; Nielsen, T. B.; McCort, S. M.; Calvert, J. M. *J. Am. Chem. Soc.* **1992**, *114*, 8435−8442. (d) Balachander, N.; Sukenik, C. N. *Langmuir* **1990**, *6*, 1621−1627. (d) Hu, J.; Wang, M.; Weier, H. U. G.; Frantz, P.; Kolbe, W.; Ogletree, D. F.; Salmeron, M. *Langmuir* **1996**, *12*, 1697−1700.

(25) Vansant, E. F.; van der Voort, P. K.; Vrancken, C. *Characterization and Chemical Modification of the Silica Surface*; Elsevier: Amsterdam, 1995; Vol. 93, Chapters 8 & 9.

(26) (a) Yoshida, W.; Castro, R. P.; Jou, J.-D.; Cohen, Y. *Langmuir* **2001**, *17*, 5882−5888. (b) Krasnoslobodtsev, A. V.; Smirnov, S. N. *Langmuir* **2002**, *18*, 3181−3184.

(27) Horr, T. J.; Arora, P. S. *Colloids Surf., A* **1997**, *126*, 113−121.

(28) Stevens, M. J. *Langmuir* **1999**, *15*, 2773−2778.

(29) Haller, I. *J. Am. Chem. Soc*. **1978**, *100*, 8050−8055.

(30) (a) Durfor, D. N.; Turner, D. C.; Georger, J. H.; Peek, B. M.; Stenger, D. A. *Langmuir* **1994**, *10*, 148−152. (b) Petri, D. F. S.; Wenz, G.; Schunk, P.; Schimmel, T. *Langmuir* **1999**, *15*, 4520−4523.

(31) Brandow, S. L.; Chen, M.-S.; Aggarwal, R.; Ducley, C. S.; Calvert, J. M.; Dressick, W. J. *Langmuir* **1999**, *15*, 5429−5432.

(32) Greene, T. W. *Protective Groups in Organic Chemistry*; Wiley-Interscience: New York, 1981; Chapter 7.

(33) Heid, S.; Effenberg, F.; Bierbaum, K.; Grunze, M. *Langmuir* **1996**, *12*, 2118−2120.

(34) Kobayashi, S.; Nishikawa, T.; Takenobu, T.; Mori, S.; Shimoda, T.; Mitani, T.; Shimotani, H.; Yoshimoto, N.; Ogawa, S.; Iwasa, Y. *Nat. Mater.* **2004**, *3*, 317−322.

(35) Vilan, A.; Shanzer, A.; Cahen, D. *Nature* **2000**, *404*, 166−168.

(36) Prutton, M. *Introduction to Surface Physics*; Oxford University Press: Oxford, 1994.

(37) Becke, A. D. *J. Chem. Phys.* **1993**, *98*, 5648−5652.

(38) Lee, C.; Yang, W.; Parr, R. G. *Phys. Rev. B* **1988**, *37*, 785−789.

(39) Frisch, M. J.; Trucks, G. W.; Schlegel, H. B.; Scuseria, G. E.; Robb, M. A.; Cheeseman, J. R.; Zakrzewski, V. G.; Montgomery, J. A., Jr.; Stratmann, R. E.; Burant, J. C.; Dapprich, S.; Millam, J. M.; Daniels, A. D.; Kudin, K. N.; Strain, M. C.; Farkas, O.; Tomasi, J.; Barone, V.; Cossi, M.; Cammi, R.; Mennucci, B.; Pomelli, C.; Adamo, C.; Clifford, S.; Ochterski, J.; Petersson, G. A.; Ayala, P. Y.; Cui, Q.; Morokuma, K.; Malick, D. K.; Rabuck, A. D.; Raghavachari, K.; Foresman, J. B.; Cioslowski, J.; Ortiz, J. V.; Stefanov, B. B.; Liu, G.; Liashenko, A.; Piskorz, P.; Komaromi, I.; Gomperts, R.; Martin, R. L.; Fox, D. J.; Keith, T.; Al-Laham, M. A.; Peng, C. Y.; Nanayakkara, A.; Gonzalez, C.; Challacombe, M.; Gill, P. M. W.; Johnson, B. G.; Chen, W.; Wong, M. W.; Andres, J. L.; Head-Gordon, M.; Replogle, E. S.; Pople, J. A. *Gaussian 98*, Revision A.7 ed.; Gaussian, Inc: Pittsburgh, PA, 1998.

(40) (a) Dunning, T. H., Jr. *J. Chem. Phys.* **1989**, *90*, 1007−1023. (b) De Proft, F.; Martin, J. M. L.; Geerlings, P. *Chem. Phys. Lett.* **1996**, *250*, 393−401.

(41) See http://www.cscs.ch/molekel/.

(42) Heise, A.; Stamm, M.; Rauscher, M.; Duschner, H.; Menzel, H. *Thin Solid Films* **1998**, *199*, 327−329.

(43) March, J. *Advanced Organic chemistry*, 4th ed.; Wiley-Interscience: New York, 1992; Chapter 0-58.

(44) Wolfe, S.; Hasan, S. K. *Can. J. Chem.*, **1970**, *48*, 3572−3579.

(45) Osby, J. O.; Martin, M. G.; Ganem, B. *Tetrahedron Lett.* **1984**, *25*, 2093−2096.

(46) Heise, A.; Menzel, H.; Yim, H.; Foster, H. D.; Wieringa, R. H.; Schouten, A. J.; Erb, V.; Stamm, M. *Langmuir* **1997**, *13*, 723−728.

(47) Oliveira, O. N.; Taylor, D. M.; Lewis, T. J.; Salvagno, S.; Stirling, C. J. M. *J. Chem. Soc., Faraday Trans. 1* **1989**, *85*, 1009−1018.

(48) The dipole moment direction is graphed from plus to minus.

(49) Chosen to be 2.5 for the calculations, as is found in references to be between 2 and 3. See ref 7 and (a) Takahagi, T.; Saiki, A.; Sakaue, H.; Shingubara, S. *Jpn. J. Appl. Phys., Part 1* **2003**, *42*, 157−161. (b) Gu, D.; Sistiabudi, R.; Dey, S. K. *J. Appl. Phys.* **2005**, *97*, 123710. (c) Campbell, L. H.; Kress, J. D.; Martin, R. L.; Smith, D. L.; Barashkov, N. N.; Ferraris, J. P. *Appl. Phys. Lett.* **1997**, *71*, 3528−3530.

(50) Bruening, M.; Cohen, R.; Guillemoles, J. F.; Moav, T.; Libman, J.; Shanzer, A.; Cahen, D. *J. Am. Chem. Soc.* **1997**, *119*, 5720−5728.

(51) Allena, G. C.; Sorbelloa, F.; Altavilla, C.; Castorina, A.; Ciliberto, E. *Thin Solid Films* **2005**, *483*, 306−311.